

LOW-DIMENSIONAL FEEDBACK CONTROL OF THE VON KARMAN VORTEX STREET AT A REYNOLDS NUMBER OF 100

Stefan Siegel, Kelly Cohen, Thomas McLaughlin
US Air Force Academy

Abstract: The effect of feedback flow control on the wake of a circular cylinder at a Reynolds number of 100 is investigated in direct numerical simulation. Our control approach uses a low dimensional model based on proper orthogonal decomposition (POD). The controller applies linear proportional and differential feedback to the estimate of the first POD mode. Actuation is implemented by displacing the cylinder normal to the flow. The closed loop feedback simulations explore the effect of both fixed phase and variable phase feedback on the wake. While fixed phase feedback is effective in reducing drag and unsteady lift, it fails to stabilize once the low drag state has been reached. Variable phase feedback, however, achieves the same drag and unsteady lift reductions while being able to stabilize the flow in the low drag state. In the low drag state, the near wake is entirely steady, while the far wake exhibits vortex shedding at a reduced intensity. We achieved a drag reduction of close to 90% of the vortex-induced drag, and also lowered the unsteady lift force by an order of magnitude.

Key words: Feedback Flow Control, Circular Cylinder, Wake, Vortex Shedding, Drag Reduction

1. INTRODUCTION

Two-dimensional bluff body wakes have been investigated for quite some time. In a two-dimensional cylinder wake, self-excited oscillations in the form of periodic shedding of vortices are observed above a critical Reynolds number of approximately 47 (Williamson (1996)). This behavior is

referred to as the von Kármán Vortex Street. According to Williamson (1996), the regime of laminar vortex shedding extends to a Reynolds number of approximately 180, before three-dimensional instabilities occur. This is the Reynolds number regime that we target in this investigation. However, the Kármán vortex street as the fundamental feature of this type of wake flow is sustained to very large Reynolds numbers (on the order of millions). Therefore the lessons learned at low Reynolds numbers will still be applicable to applications of practical interest at much higher Reynolds numbers. Conversely, it would be impossible to control the flow at high Reynolds numbers without being able to successfully do so at low Reynolds numbers.

The non-linear oscillations of the vortex street lead to some undesirable effects associated with unsteady pressures such as fluid-structure interactions (Roussopoulos(1993)) and lift/drag fluctuations (Park et al. (1994)). Examples of real life applications subject to these are wakes of submarine turrets, ocean drilling rigs, and flame holders in turbine engines. Also, the vortices themselves greatly increase the drag of the bluff body, compared to the steady wake that can be observed at lower Reynolds numbers. Monkewitz (1996) showed that the von Kármán Vortex Street is the result of an absolute, global instability in the near wake of the cylinder. Further downstream the flow is convectively unstable. This absolute instability is causing the flow to behave as a self sustained oscillator, with internal positive feedback leading to temporal amplification of the oscillation by the recirculation region downstream of the cylinder.

2. NUMERICAL METHODS

The goal of this paper is to apply the approach developed by Cohen et al. (2003) to a full Navier Stokes simulation of the flow field. A schematic of this approach is shown in Figure 1.

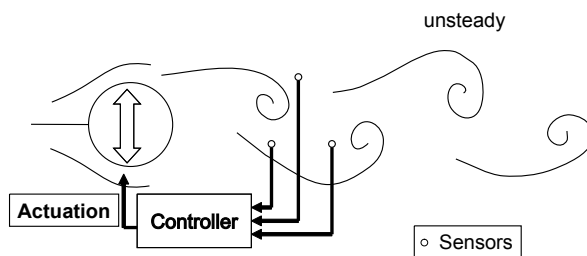


Figure 1. Setup of Simulation and Sensors

A limited number of sensors ($n > 1$) are used to estimate the state of the flow which is characterized using a low dimensional model. The controller then acts on the flow state estimates in order to determine the actuator displacement (Figure 1 shows the overall setup of this experiment).

2.1 CFD Model

For the numerical simulations, Cobalt Solutions' Cobalt solver V.2.02 running on a Beowulf cluster was used. This code can operate in many different modes using various turbulence models, however, for the present investigation it was used as a direct Navier Stokes solver with second order accuracy in time and space. Cobalt operates on unstructured grids, for all investigations an unstructured two-dimensional grid with 63700 Nodes / 31752 Elements was used. The grid extended from -16.9 cylinder diameters to 21.1 cylinder diameters in the x (streamwise) direction, and ± 19.4 cylinder diameters in y (flow normal) direction.

The Strouhal number obtained from the COBALT CFD model used in this effort is $St = 0.163$ at $Re = 100$ which compares well with the reported literature (Williamson (1996)).

2.2 POD Modeling and Estimation

Feasible real time estimation and control of the cylinder wake may be effectively realized by reducing the model complexity of the cylinder wake as described by the Navier-Stokes equations, using POD techniques. POD, a non-linear model reduction approach is also referred to in the literature as the Karhunen-Loeve expansion (Holmes et al. 1996). The desired POD model contains an adequate number of modes to enable modeling of the temporal and spatial characteristics of the large-scale coherent structures inherent in the flow.

In this effort, the method of "snapshots" introduced by Sirovich (1987) is employed to generate the basis functions of the POD spatial modes from the numerical solution of the Navier-Stokes equations obtained using COBALT. In all 200 snapshots were used equally spaced at 0.00735 seconds apart. The time between snapshots is five times the simulation time step. The snapshots were taken after ensuring that the cylinder wake reached steady state. This decision was made in order to be able to estimate the mode amplitudes based on sensor information, which will yield the U and V component of velocity. Since the change in mean flow distribution is an important quantity, we chose the U velocity component over the V velocity component. We

found that more than 99.98% of the kinetic energy of the flow lies in the first eight modes, with more than 90% in the first four modes. The POD algorithm was applied to the fluctuating velocity component in the direction of the flow as described in Equation (1). The decomposition of this component of the velocity field is as follows:

$$\tilde{u}(x, y, t) = U(x, y) + u(x, y, t) \quad (1)$$

where U [m/s] denotes the mean flow velocity and u [m/s] is the fluctuating component that may be expanded as:

$$u(x, y, t) = \sum_{k=1}^n a_k(t) \phi_i^{(k)}(x, y) \quad (2)$$

where $a_k(t)$ denotes the time-dependent coefficients having units of m/s and $\phi(x, y)$ represent the non-dimensional spatial Eigenfunctions determined from the POD procedure. Once the spatial POD Eigenfunctions have been derived, the corresponding time-dependent coefficients $a_k(t)$, or mode amplitudes, need to be calculated. For this, two different schemes are reported in literature. Most often a Galerkin projection is used, which involves projecting the spatial Eigenfunctions onto the Navier Stokes equations. This process involves spatial derivatives of the snapshots, which are, particularly in the case of experimental data, inherently sensitive to noise. Gillies (1995) used a simple least squares fit, which we found to be much more effective.

The sensor grid employed for all simulations employs a total of 35 sensors in the near wake of the cylinder. The main advantage of this sensor grid over others investigated is in its ability to provide a global estimate of the mode amplitudes that shows little error compared to using all grid points. This holds true both for the unforced case as well as the feedback controlled cases. Typical errors of mode estimates are negligible in phase and less than 5 % in amplitude.

2.3 Controller

The Cobalt CFD solver has the ability to perform rigid body motion of a given grid. This feature was used to perform both time periodically forced and feedback controlled simulations with a single actuator. For all investigations, only displacement of the cylinder in flow normal (y) direction was employed for forcing the flow. Following earlier developments the control algorithm acts on the estimate of the Mode 1 amplitude only (Cohen

et al. (2003)). This design decision was made based on our earlier investigations controlling a low dimensional model of the flow. For the low dimensional model, proportional gain applied to Mode 1 only was sufficient to suppress vortex shedding. Our CFD simulations require a filter to avoid feeding back of small amounts of noise. Furthermore, we employed a Proportional and Differential (PD) feedback control strategy (Figure 2).

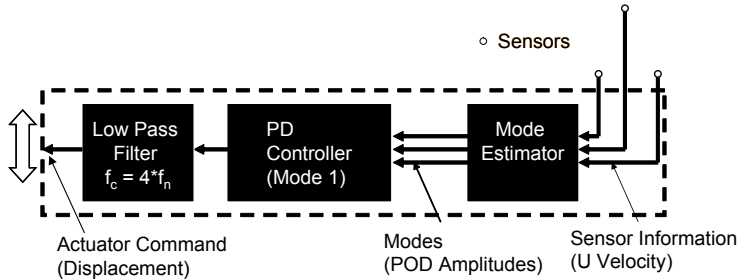


Figure 2. Controller Schematic

Physically, the control algorithm was implemented in Matlab on a separate PC running Windows. It interfaced to the Beowulf cluster running Cobalt using Windows file sharing through Samba in order to read the sensor information and provide commands to update the cylinder displacement.

3. RESULTS

Before closed loop feedback flow control is employed, it is important to investigate the dynamics of the unforced flow field in detail. Equally important, the effect of open loop forcing needs to be understood, since the receptivity of the flow to forcing will manifest itself in these investigations. The following section will outline the results of these investigations, and also show the limitations of the type of forcing employed as well as the limits of the flow improvements that may be obtained using feedback control.

The following sections will highlight one select case of feedback flow control. We investigated two different methods of feedback control, one using a fixed set of proportional and differential gains, and one set where the gains were varied depending on the change in the mean flow. The latter is usually referred to as a gain scheduling scheme, and showed better results in stabilizing the wake. The most successful fixed gain feedback cases were

able to achieve as much drag reduction as the variable gain feedback, but failed to stabilize the flow in the low drag state. In the context of this paper we will only discuss the variable gain strategy results in detail, for further details on the fixed gain investigations refer to Siegel et al. (2003).

3.1 Unforced and open loop results

In a CFD simulation, the flow field is started abruptly at time zero. The flow evolves from a Stokes-type streamline pattern at the start of the simulation through a steady wake with two closed recirculation bubbles into the unsteady von Kármán Vortex Street. During this startup, the flow reaches a state of minimum drag. It is worth noting that the minimum drag does not coincide in time with the steady wake as one might expect, but rather with a vortex shedding pattern with a very large wavelength. The total drag in this situation is about 16 % less than in the steady state vortex shedding situation. Thus one may argue that a feedback control scheme aiming to suppress the vortex shedding may be able to recover up to this portion of the total drag, at best. We refer to this portion of the overall drag force as the *vortex induced drag*, since it is caused by the vortex shedding in the unsteady wake flow. It is a portion of the pressure drag. After about 10 shedding periods after the startup of the simulation, the wake approaches a time periodic vortex shedding state. The mean recirculation zone ends at $x/D = 1.9$ in this flow state.

The cylinder wake flow can be forced in an open loop fashion using sinusoidal displacement of the cylinder with a given amplitude and frequency. Koopman (1967) investigated the response of the flow to this type of forcing in a wind tunnel experiment. He found a region around the natural vortex shedding frequency where he could achieve “lock-in”, which is characterized by the wake responding to the forcing by establishing a fixed phase relationship with respect to the forcing. The frequency band around the natural vortex shedding frequency for which lock-in may be achieved is amplitude dependent. In general, the larger the amplitude, the larger the frequency band for which lock-in is possible. However, a minimum threshold amplitude exists below which the flow will no longer respond to the forcing any more. In Koopman’s experiment, this amplitude was at 10% peak displacement of the cylinder.

We resampled the lock-in region in the CFD simulation at select amplitude and frequency pairs. The simulations activated the forcing always at the same time, 3.3 seconds after the start of the simulation, which resulted in the forcing being 180 degrees out of phase with the vortex shedding. The flow field goes through a transient phase before lock-in is achieved after a certain number of shedding cycles. We refer to the time during which the

flow adjusts to the forcing as the settling time. A scan through different forcing amplitudes was performed at the natural shedding frequency with amplitudes ranging from 1 to 30 % of the cylinder diameter. The settling times observed in these cases are shown in Figure 3. While the settling times are roughly constant down to a forcing amplitude of 5%, for smaller amplitudes a drastic increase in settling times can be observed. This manifests the behavior observed by Koopman around 10% forcing amplitude, albeit shifted towards somewhat smaller amplitudes. There are two possible explanations for this. Koopman used spanwise coherence as an indicator for lock-in, which may occur at larger amplitudes than the local lock-in observed in our two-dimensional simulations. Additionally, his experiment was conducted in a wind tunnel environment which features more mean flow turbulence than the CFD simulations. This would also tend to increase the amount of forcing needed to overcome the turbulence and achieve lock-in.

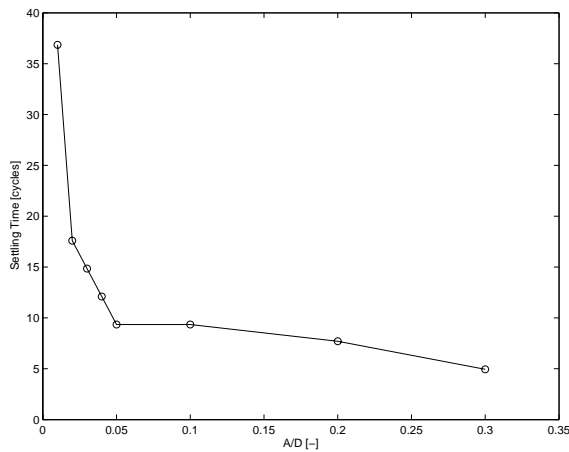


Figure 3. Open loop forcing settling time

Shifting the forcing frequency away from the natural shedding frequency yields a qualitatively different behavior, ultimately yielding a chaotic flow behavior at and beyond the lock-in limit according to Koopman. We were able to verify this behavior in the simulation.

The open loop forcing results have important implications for the closed loop feedback control runs. Since our POD model is based on unforced flow field data, it can only capture flow behavior that is phenomenologically similar to the unforced wake. In terms of the lock-in region, this flow behavior is encountered as long as the controller keeps the flow within the

lock-in region. The chaotic behavior at off-natural frequencies is clearly not modeled in the POD modes. Also, more importantly, if the displacement of the cylinder becomes smaller than about 5% of the cylinder diameter, the flow will no longer be responsive to the forcing.

3.2 Variable Phase Feedback

During an investigation into different sensor configurations, we used a sensor field with 35 sensors localized between $x/D = 0.75$ and $x/D 1.75$. As was later discovered, this sensor field developed a large estimation error with respect to the phase error of the Mode 1 estimate, when compared to an estimate based on the entire flow field, as shown in Figure 4.

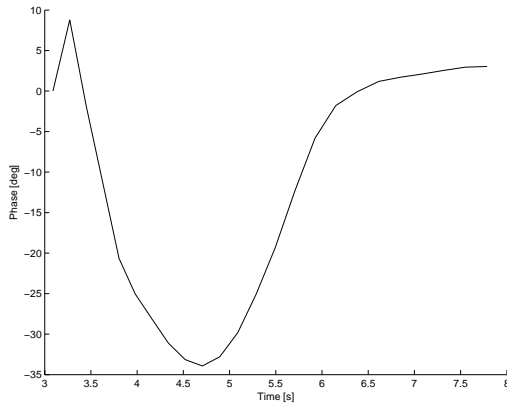


Figure 4. Feedback phase during feedback controlled run.

Nonetheless, this phase error led to a stabilization of the wake at a drag reduction of about 15% with an unsteady lift amplitude reduction of 90%, compared to the unforced flow field (Figure 5). Inspecting the phase error, one can see that due to the effects of the local sensor field the phase advance is reduced to almost zero in the steady state case. This phase advance angle stabilizes the flow field at a low level of vortex shedding, with the recirculation length extended to $x/D = 3.95$, or more than twice the unforced length.

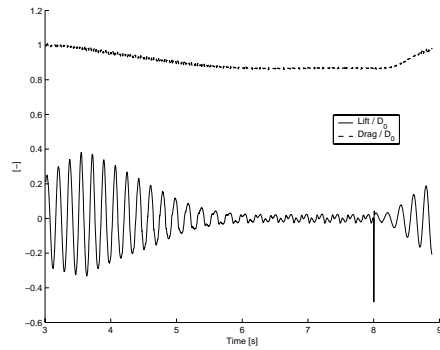


Figure 5. Lift and Drag using variable phase feedback control. The controller is activated at 3.01 s and deactivated at 8 s

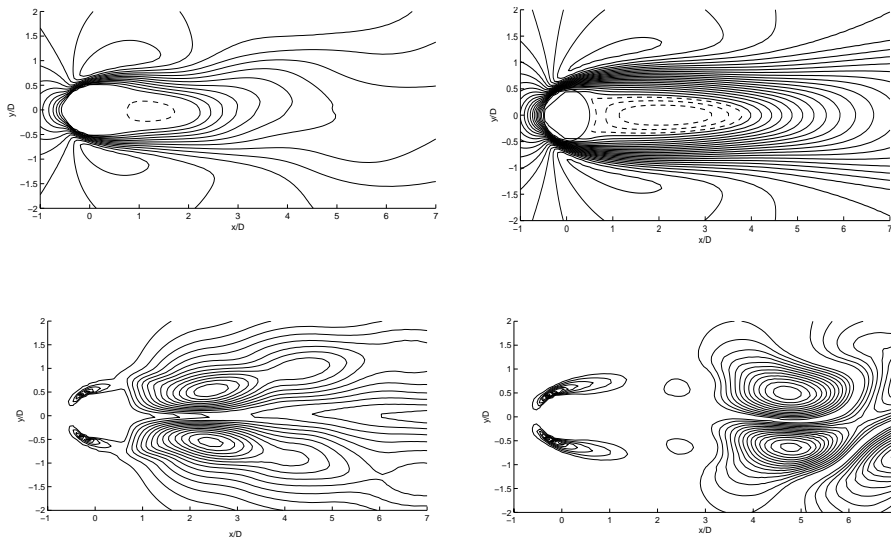


Figure 6. Mean flow (top) and RMS velocity distributions (bottom). Left, uncontrolled, right, controlled case. The cylinder is centered at (0,0) and of diameter 1, flow from left to right. Negative isocontours are dashed, positive isocontours are solid lines.

While in the simulation shown in Figures 3-6 the phase advance was a result of the sensor placement, the same effect can be achieved using a global sensor field in combination with a variable phase advance based on the non - fluctuating mean flow mode. Thus we find that a variable gain

strategy that adjusts the feedback gains according to the change in the mean flow achieves better results than a fixed gain control approach.

The drag and unsteady lift force reduction manifests itself in a change in the mean flow, as well as the RMS distribution. Figure 5 compares the unforced mean flow and RMS distributions to those encountered in the stabilized state, between 6 and 8 seconds, in the feedback controlled run. The recirculation zone length has almost doubled in length, and the peak in the RMS distribution is shifted from $x/D=2.5$ to $x/D = 5$. Also, it can be seen that the wake up to 3 diameters downstream of the cylinder is entirely steady.

3.3 Stability Analysis of Feedback Controlled Flow

When applying feedback control, significant changes in the mean flow field occur, as shown in the previous section. It is therefore of interest to investigate how the stability characteristics of the mean flow are modified as a result of the mean flow changes. Linear stability analysis based on numerical solution of the Orr-Sommerfeld equations using spectral methods (Trefelthen (2000)) was used to analyze these changes.

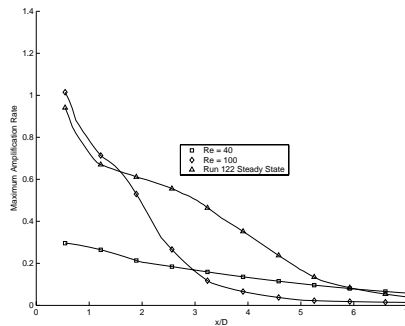


Figure 7. Linear stability analysis of unforced and feedback controlled flow fields

Figure 7 compares the maximum growth rate of the unforced flow field at a Reynolds number of 100 to the steady state feedback controlled flow field (Run 122). Despite the fact that the near wake fluctuations are suppressed by the feedback as shown in the previous section, the flow field has become more unstable beyond two diameters downstream of the cylinder. Comparing the unforced flow to a stable flow field at a subcritical Reynolds number of 40, one can see that the Karman vortex street at $Re = 100$ leads to a more stable flow field beyond $x/D = 3$.

4. DISCUSSION

We used Proper Orthogonal Decomposition (POD) as a tool to process multiple sensor signals into a global estimate of the flow state. POD allows for stable global wake state estimates, enables multi sensor evaluation and eliminates artifacts of local sensing, i.e. sensing at nodes of the vortex street. It also allows for an accurate state estimate when the effect of the controller causes major changes both in the mean flow and the rms amplitudes of the fluctuating velocity components. However, we find it necessary to account for the changes in the mean flow by adding a mean flow mode to the model.

While we used only Mode 1 for closing the feedback loop, all the higher order POD modes experienced proportional reductions in mode amplitude. This suggests a strong coupling between all modes, and implies that the existence of the higher order modes is conditional on the presence of the fundamental modes. This confirms the results of our previous work (Cohen et al. (2003)).

While feedback control was able to stabilize the near wake of the cylinder, vortex formation still occurred further downstream. While the reasons for this are not entirely clear, we suggest several possible causes. The change in the mean flow caused by the controller lengthens the recirculation zone. This moves the vortex formation location further downstream and causes a reduction in both drag and rms lift force. While both of these effects are desired, the downstream shift in vortex formation location causes a larger spatial separation between the actuation, which remains at the cylinder, and the oscillations the actuator attempts to cancel. This requires both more actuation input, and also an adjustment in the actuation phase in order to account for the time a given disturbance takes to travel from the actuator to the vortex formation location. At the same time the disturbances caused by the actuator need to travel through a region of the flow which, while stabilized, is only stabilized within a narrow range of phase angles. If the far wake requires a phase angle for stabilization that at the same time destabilizes the near wake, a physical limit has been reached in terms of what can be achieved given the actuator location. This effect may limit the spatial range for which stabilization can be achieved with the current actuator setup.

Despite all these problems, we were able to suppress the oscillations in the near wake without actively modifying the mean flow or changing the separation point using for example momentum injection. Thus this effort shows that the cylinder wake flow can be improved in terms of drag and unsteady lift by feedback control. For this reason, one would expect the current control approach to be applicable to wake flows with fixed

separation points, like the flow around a D- shaped cylinder. The same cannot be said for approaches that aim at moving the separation point aft, for example by tripping the boundary layer or using blowing and suction upstream of the separation point to delay separation.

Overall, we were able to reduce the effect of vortex shedding on both the unsteady lift and the vortex induced (pressure) drag by about an order of magnitude.

5. ACKNOWLEDGMENTS

The authors would like to acknowledge funding for this research from the Air Force Office of Scientific Research, program monitor Dr. Belinda King. We would also like to acknowledge the fruitful discussions and information exchange with Gilead Tadmor and Bernd Noack.

6. REFERENCES

- Williamson, C.H.K., "Vortex Dynamics in the Cylinder Wake", *Ann. Rev. Fluid Mech.*, 1996, 28:477-539
- Roussopoulos, K., "Feedback control of vortex shedding at low Reynolds numbers", *Journal of Fluid Mechanics*, Vol. 248, 1993, pp. 267-296.
- Park, D. S., Ladd, D. M., and Hendricks, E. W., "Feedback control of von Kármán vortex shedding behind a cylinder at low Reynolds numbers", *Phys. Fluids*, Vo. 6, No.7, 1994, pp. 2390-2405.
- Monkewitz, P. A., "Modeling of self-excited wake oscillations by amplitude equations", *Experimental Thermal and Fluid Science*, Vol. 12, 1996, pp. 175-183.
- Koopmann, G., "The Vortex Wakes of Vibrating Cylinders at Low Reynolds Numbers", *Journal of Fluid Mechanics*, Vol. 28 Part 3, 1967, pp. 501-512.
- Gillies, E. A., "Low-dimensional characterization and control of non-linear wake flows", PhD. Dissertation, University of Glasgow, Scotland, June 1995.
- Cohen, K., Siegel, S., McLaughlin, T., Gillies, E., "Feedback Control of a Cylinder Wake Low Dimensional Model", *AIAA Journal*, Vol 41, No.8, August 2003 (Tentative).
- Holmes, P., Lumley, J. L., and Berkooz, G., "Turbulence, Coherent Structures, Dynamical Systems and Symmetry", Cambridge University Press, Cambridge, Great Britain, 1996, pp. 86-127.
- Sirovich, L., "Turbulence and the Dynamics of Coherent Structures Part I: Coherent Structures", *Quarterly of Applied Mathematics*, Vol. 45, No. 3, 1987, pp. 561-571.
- Siegel, S, Cohen, K., McLaughlin, T. "Feedback Control of a Circular Cylinder Wake in Experiment and Simulation" *AIAA Paper* 2003-3569, June 2003.
- Trefelthen, L.N., "Spectral Methods in MATLAB", *SIAM*, Philadelphia, PA, 2000, pp. 145-152